MT-L1529-6

TECHNICAL REPORT

EVALUATION OF A FAILED RIVERWATER PUMP SHAFT COUPLING FROM THE BEAVER VALLEY POWER PLANT

C. J. CZAJKOWSKI

JUNE 1992

Nuclear Waste and Materials Technology Division

DEPARTMENT OF NUCLEAR ENERGY, BROOKHAVEN NATIONAL LABORATORY
UPTON, NEW YORK 11973

Prepared for the U.S. Nuclear Regulatory Commission
Office of Nuclear Reactor Regulation
Contract No. DE-AC02-76CH00016

EVALUATION OF A FAILED RIVERWATER PUMP SHAFT COUPLING FROM THE BEAVER VALLEY POWER PLANT

C. J. CZAJKOWSKI

JUNE 1992

Nuclear Waste and Materials Technology Division
Department of Nuclear Energy
Brookhaven National Laboratory
Associated Universities, Inc.
Upton, New York 11973

This work was performed under the auspices of the United States Nuclear Regulatory Commission
FIN L-1529

TABLE OF CONTENTS

	PAGE
LIST OF FIGURES	v
1. INTRODUCTION	1
2. VISUAL EXAMINATION/CHEMICAL ANALYSIS	1
3. OPTICAL MICROSCOPY	3
4. SCANNING ELECTRON MICROSCOPY/ENERGY DISPERSIVE SPECTROSCOPY	3
5. HARDNESS/TENSILE/CHARPY IMPACT TESTING	8
6. DISCUSSION AND CONCLUSIONS	20
7. REFERENCES	22

LIST OF FIGURES

		PAGE
Figure 1	Sketch of broken riverwater pump shaft coupling from Beaver Valley Plant.	2
Figure 2	Low magnification photograph of optical mount -A- (unetched) -B- (etched)	4
Figure 3	Higher magnification photograph showing cracks following prior austenite grain boundaries (intergranular)	5
Figure 4	This photomicrograph depicts the structure of the coupling as tempered martensite	5
Figure 5a	SEM photo of fracture showing intergranular cracking.	6
Figure 5b	The cracking in this section was also intergranular	6
Figure 5c	Definite intergranular cracking was seen in this third area examined	6
Figure 6a	Fracture after deoxidation treatment (intergranular)	7
Figure 6b	Second area also showing intergranular failure.	7
Figure 6c	Third area examined - typically intergranular	7
Figure 7	Stress-strain curves for specimens 1 and 2.	9
Figure 8	Stress-strain curves for specimens 3 and 4.	10
Figure 9a	SEM photo tensile specimen 1.	12
Figure 9b	Grain boundary decohesion is evident at higher magnification	12
Figure 10a	SEM photo of tensile specimen 4	12
Figure 10b	Higher magnification photo of specimen 4 show same type failure as seen in specimen 1 (Figure 9b).	12
Figure 11a	The fracture face from impact specimen C1 is essentially all intergranular	13
Figure 11b	Higher magnification fractograph showing intergranular features.	13
Figure 12a	The fracture face of C2 was also intergranular	13
Figure 12b	Higher magnification fractograph of C2	13

LIST OF FIGURES (cont.)

		PAGE
Figure 13a	C4 fracture face was also intergranular	14
Figure 13b	Intergranular facets are clearly evident on C4	14
Figure 14a	C6 fracture face was also essentially all intergranular	14
Figure 14b	Higher magnification fractograph of C6	14
Figure 15a	Low magnification fractograph of C7. Area A - Shear fracture; Area B - quasi cleavage area broken in liquid N_2 temperatures	15
Figure 15b	Dimpled rupture failure is characteristic of Area A	15
Figure 15c	Quasi-cleavage failure of Area B was typical	15
Figure 16a	The fracture face for C6 was almost entirely a shear fracture	17
Figure 16b	The ductile nature of the fracture is evident in this higher magnification fractograph of C6	17
Figure 17a	Low magnification photomicrograph from sample C8 - no grain boundary etching (7 minutes)	18
Figure 17b	Grain boundary etching is evident on sample C2 specimen	18
Figure 18a	No evidence of grain boundary etching at higher magnification of C8 (7 minutes)	18
Figure 18b	Grain boundaries are clearly delineated on sample C2	18
Figure 19a	Fourteen minutes of etching did not reveal grain boundaries on specimens from C8	19
Figure 19b	Grain boundaries are seen on C2 after 14 minutes of etching	19
Figure 20a	Higher magnification photo showing no boundary etching	19
Figure 20b	Grain boundaries are clearly seen on C2 at higher magnification	19

1. INTRODUCTION

In October 1991 a riverwater pump shaft coupling at the Beaver Valley Nuclear Power Plant failed during operation. The coupling was used to join two shafts of a Byron Jackson Vertical Circulator river water pump. The pump rotates at 1170 RPM in river water of 32-90°F and produces a discharge pressure of 68 psi. The coupling was provided by Byron Jackson as part of an order containing 12 identical couplings.

A preliminary root cause analysis performed by Lehigh University (for the utility) concluded that the failure occurred due to an improper heat treatment being applied to the 410 stainless steel couplings which resulted in a temper embrittled condition (making the component susceptible to cracking).

In order to independently evaluate the failure, the U.S. Nuclear Regulatory Commission (NRC) requested Brookhaven National Laboratory (BNL) to perform a metallurgical failure analysis on a failed coupling from Beaver Valley.

This investigation consisted of:

a) Visual Examination/Chemical Analysis
b) Optical Microscopy
c) Scanning Electron Microscopy (SEM)
d) Hardness/Tensile/Charpy Impact Testing

This report documents the results of the failure investigation.

2. VISUAL EXAMINATION/CHEMICAL ANALYSIS

A broken coupling (Figure 1) was received at BNL. The coupling had been sectioned into six pieces by Lehigh University personnel prior to shipment.

Visual inspection of the pieces showed an oxide coating on the fractures and the appearance of worn threads on the inside surface of the coupling. Various sections were cut from the fracture face for SEM evaluation, while other sections were cut for the mechanical and chemical analysis specimens.

Samples sent out for chemical analysis yielded the following results:

TABLE 1 Chemical Analysis Results

Element	Wt. %	AISI 410 Requirements Wt. %
Carbon	0.12	0.15 max
Manganese	0.42	1.00 max
Silicon	0.41	1.00 max
Nickel	0.55	No requirement
Chromium	12.02	11.5 - 13.5
Sulfur	0.012	0.030 max
Phosphorous	Not Tested	0.040 max

The results are consistent with those of a typical 410 stainless steel.

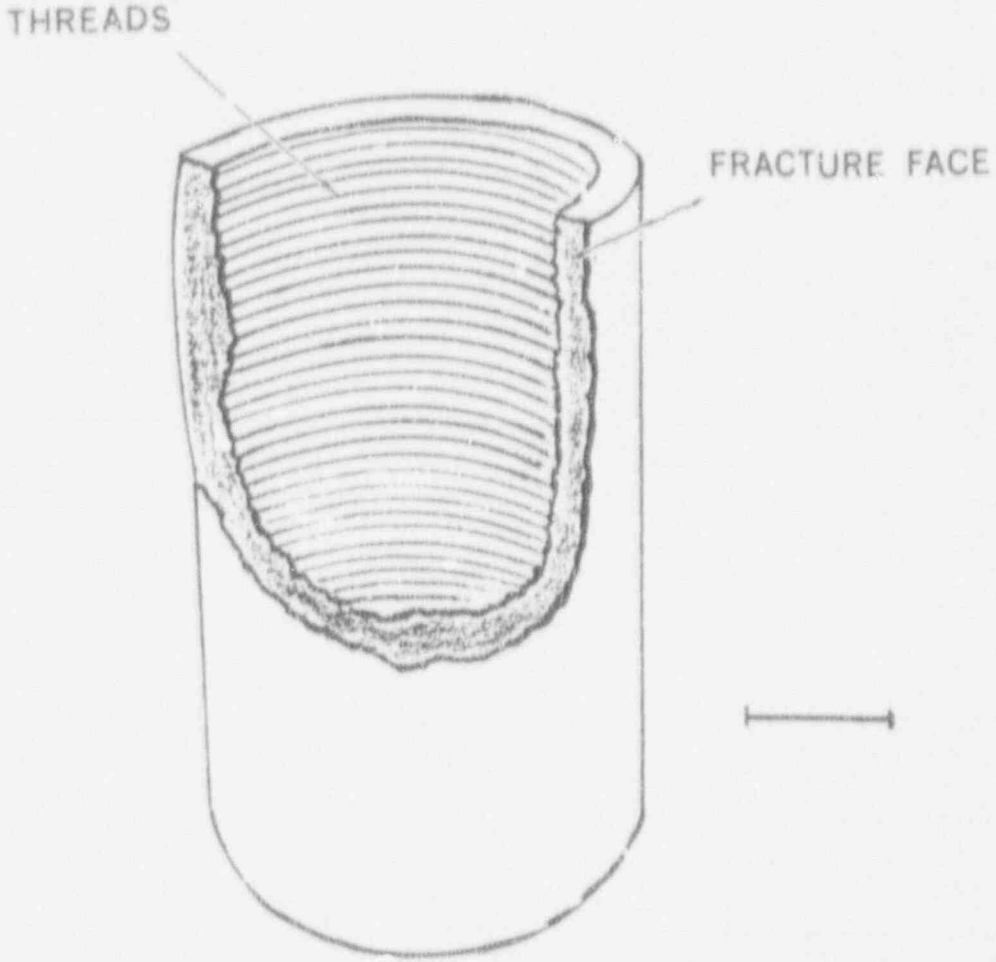

Figure 1 Sketch of broken riverwater pump shaft coupling from Beaver Valley Plant.

3. OPTICAL MICROSCOPY

One section was cut from the coupling which contained two cracks. This sample was mounted and then metallurgically ground and polished. The specimen was etched in an ethereal picral etch [1].

Figure 2 is a low magnification photomicrograph of the area of cracking on the mounted specimen. The crack was intergranular with the cracking following prior austenite grain boundaries as seen in Figure 3. The material structure was that of tempered martensite (Figure 4) which is typical for the 410 stainless steel alloy.

4. SCANNING ELECTRON MICROSCOPY (SEM)/ENERGY DISPERSIVE SPECTROSCOPY (EDS)

Various fracture areas were examined along the fracture face of the crack (Figure 1). The fracture surfaces were covered by an oxide film (Figures 5a-c) and were definitely intergranular. After initial examination, the specimens were deoxidized using an electrolytic process as follows:

A working solution of Endox-214 is prepared by adding 8 ounces of Endox-214 powder to 1000 ml of cold water and stirring until it is completely dissolved. A small amount of Photoflow is added to the solution to aid the wetting of the specimen and eliminate some of featuring during the electrochemical cleaning step. A glass beaker with 500 ml of Endox-214 solution is placed in an ultrasonic cleaner. The specimen is made the cathode, and a platinum wire loop is the anode. A current density of approximately 250 mA/cm^2 is applied for 15 seconds. Remove the specimen from the electrolyte and ultrasonically wash it in a detergent solution consisting of Alconox and Photoflow for one minute, then rinse in clean water, dip in methanol and dry in hot air. The above procedure comprises one cycle. It may be necessary to repeat the above cycle several times before removing all the corrosion products. It is not possible to predetermine the exact number of cleaning cycles for any given specimen, since it depends upon the severity of the oxidation, roughness of surface, and the physical size of the sample. Observe the specimen optically after each cycle so that the process can be discontinued after the oxide or the corrosion product is removed and the specimen surface looks clean. After the specimen is thoroughly dry, examine it immediately or store in a desiccator.

The specimens were reexamined after this treatment by SEM (Figures 6a-c). There was no evidence of fatigue interaction (beach marks, etc.) nor indication of other than an intergranular mode of failure.

One of the "as received" specimens was also analyzed by EDS. Four EDS scans were performed on the threaded area of the coupling (2 scans), the outside surface of the coupling and on a cut and ground cross section (bare metal) of the coupling material. There was a clear indication that chromium (Cr) was substantially higher on the interior threaded area and on the exterior coupling surface than was apparent in the cross section examined. This observation supports the hypothesis that the coupling may have been chromium plated prior to being entered into service.

Figure 2 Low magnification photograph of optical mount -A- (unetched) -B- (etched).

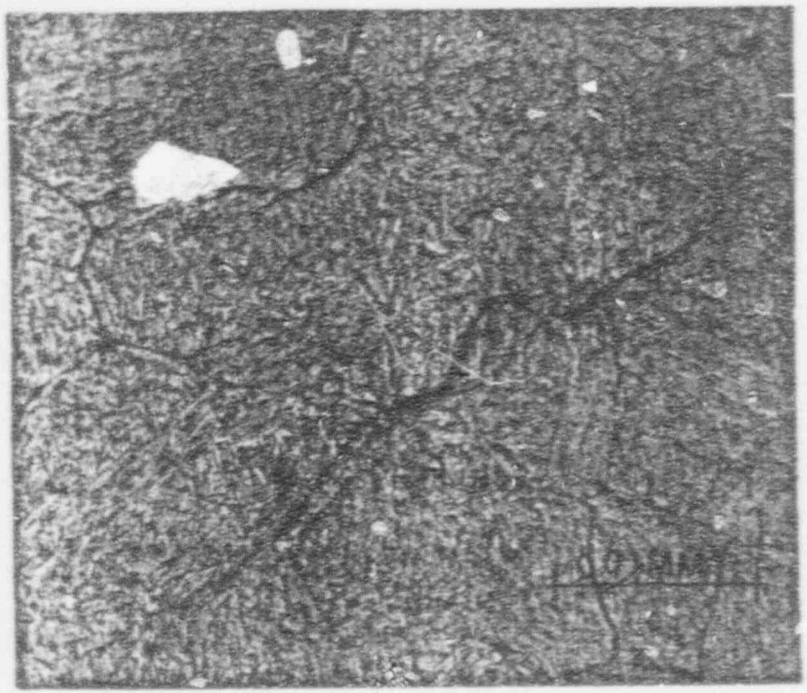

Figure 3 Higher magnification photograph showing cracks following prior austenite grain boundaries (intergranular).

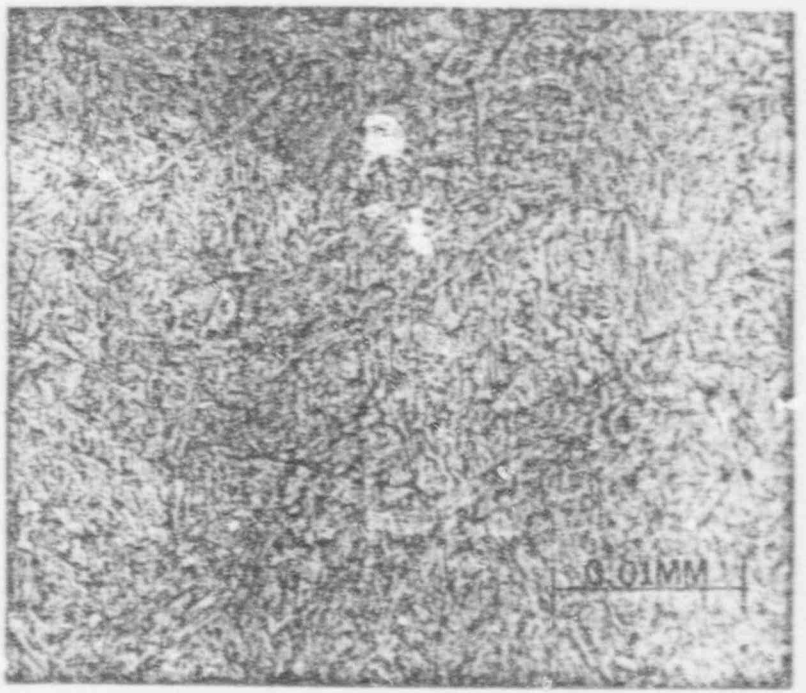

Figure 4 This photomicrograph depicts the structure of the coupling as tempered martensite.

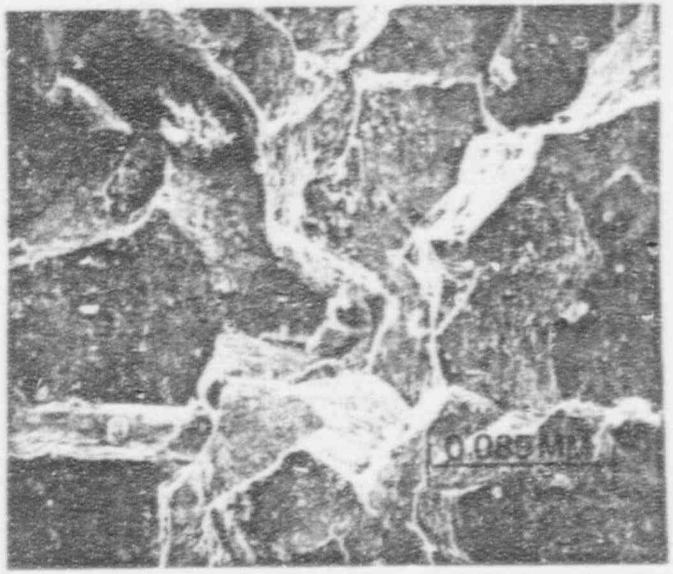

Figure 5a SEM photo of fracture showing intergranular cracking.

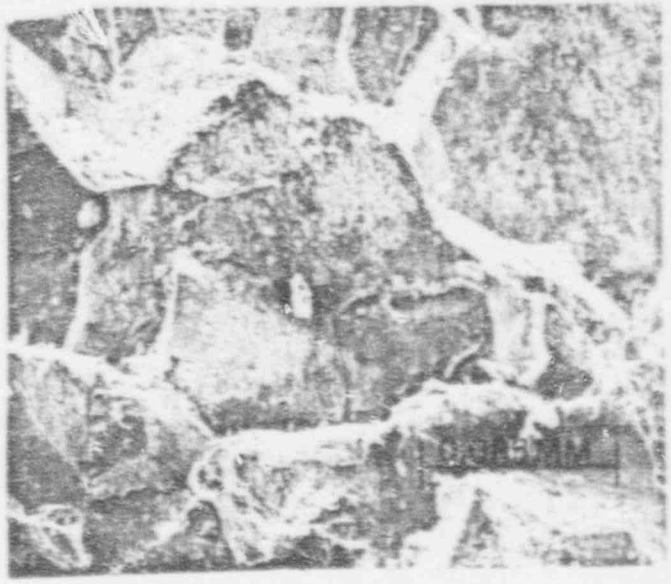

Figure 5b The cracking in this section was also intergranular.

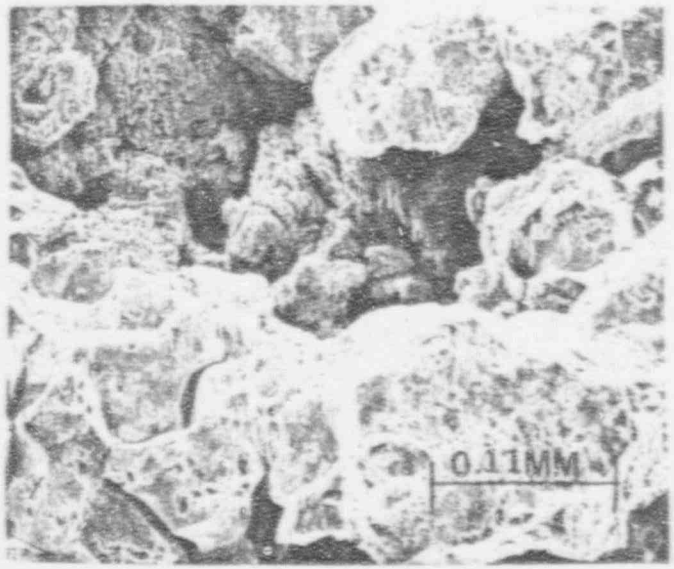

Figure 5c Definite intergranular cracking was seen in this third area examined.

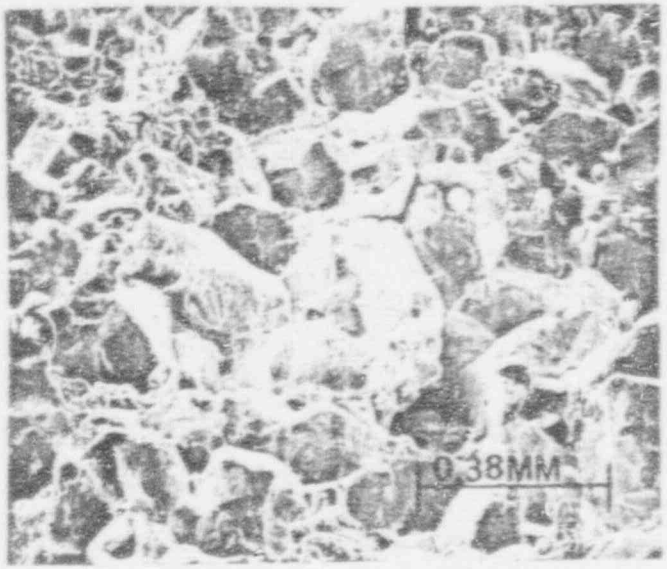

Figure 6a Fracture after deoxidation treatment (intergranular).

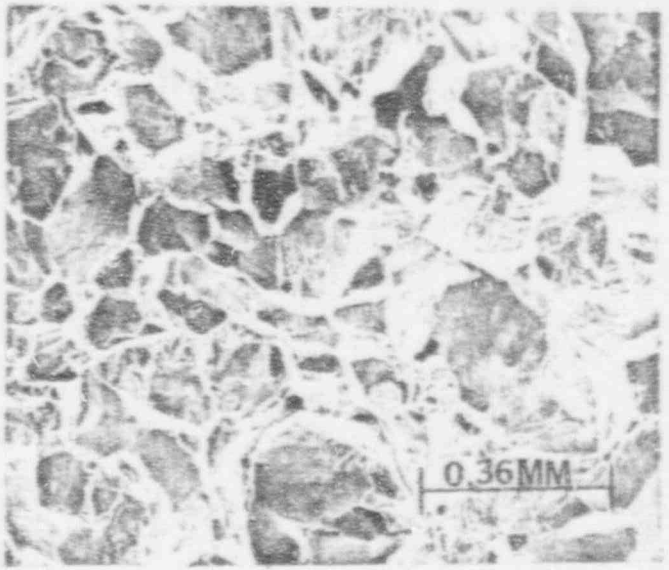

Figure 6b Second area also showing intergranular fail re.

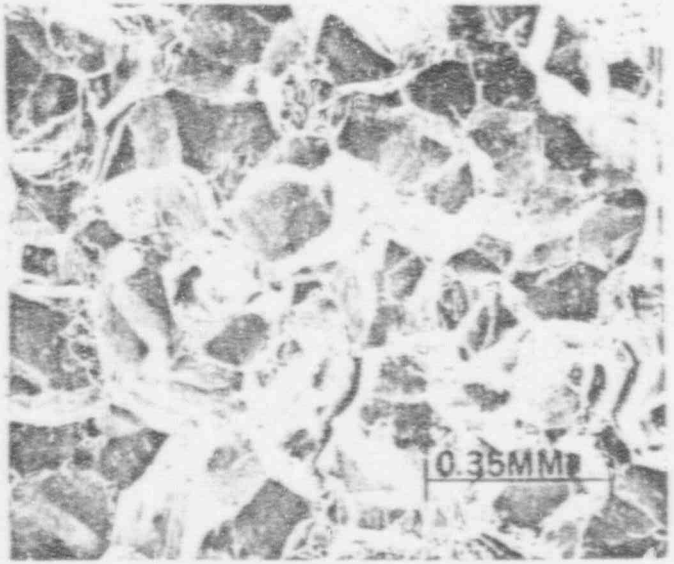

Figure 6c Third area examined - typically intergranular.

5. HARDNESS/TENSILE/CHARPY IMPACT TESTING

Hardness Testing

Nine microhardness measurements (500g load) were performed on a specimen cut from the failed coupling. The following are the measurement results (in brackets are the equivalent Rockwell "C" scale measurements):

TABLE 2 Microhardness Results

348 (33)	348 (33)	348 (33)
353 (33)	296 (24)	343 (32)
348 (33)	343 (32)	353 (33)

This averages to a R_c equivalent of 32 which would equate to a 410 stainless steel tempered at ~1000°F [2].

Tensile Testing

Four subsized tensile specimens were machined from the coupling. Figures 7 and 8 are the stress - strain curves generated from the testing. Specimens 1-3 were tested "as received", while specimen 4 had been vacuum degassed at 200°C for 48 hours prior to testing.

Table 3 tabulates the test results:

Table 3 Mechanical Test Results

Specimen Number	Ultimate Tensile Stress (psi)	Stress at 0.2% Yield (psi)	Modulus (psi)	Elongation (%)	Reduction in Area (%)
1	140600.	93660.	30240000.	14.51	67.40
2	141500.	84740.	26950000.	15.81	70.60
3	139000.	86650.	30720000.	14.74	69.40
4	143200.	89520.	29400000.	15.37	71.20
Mean	141100.	88640.	29330000.	15.11	69.65
Typical 41055	145,000	115,000	---	20	65

The tensile strength and reduction of area are very similar to that expected [2] from a 410 stainless steel tempered at 1000°F. Both the stress at 0.2% yield and the elongation were lower than that expected for the same steel.

The fracture faces from both tensile specimens 1 and four were examined under the electron microscope. Figures 9a - 10b show the results of this examination. It is evident on the fractographs that slight ductility (dimpled

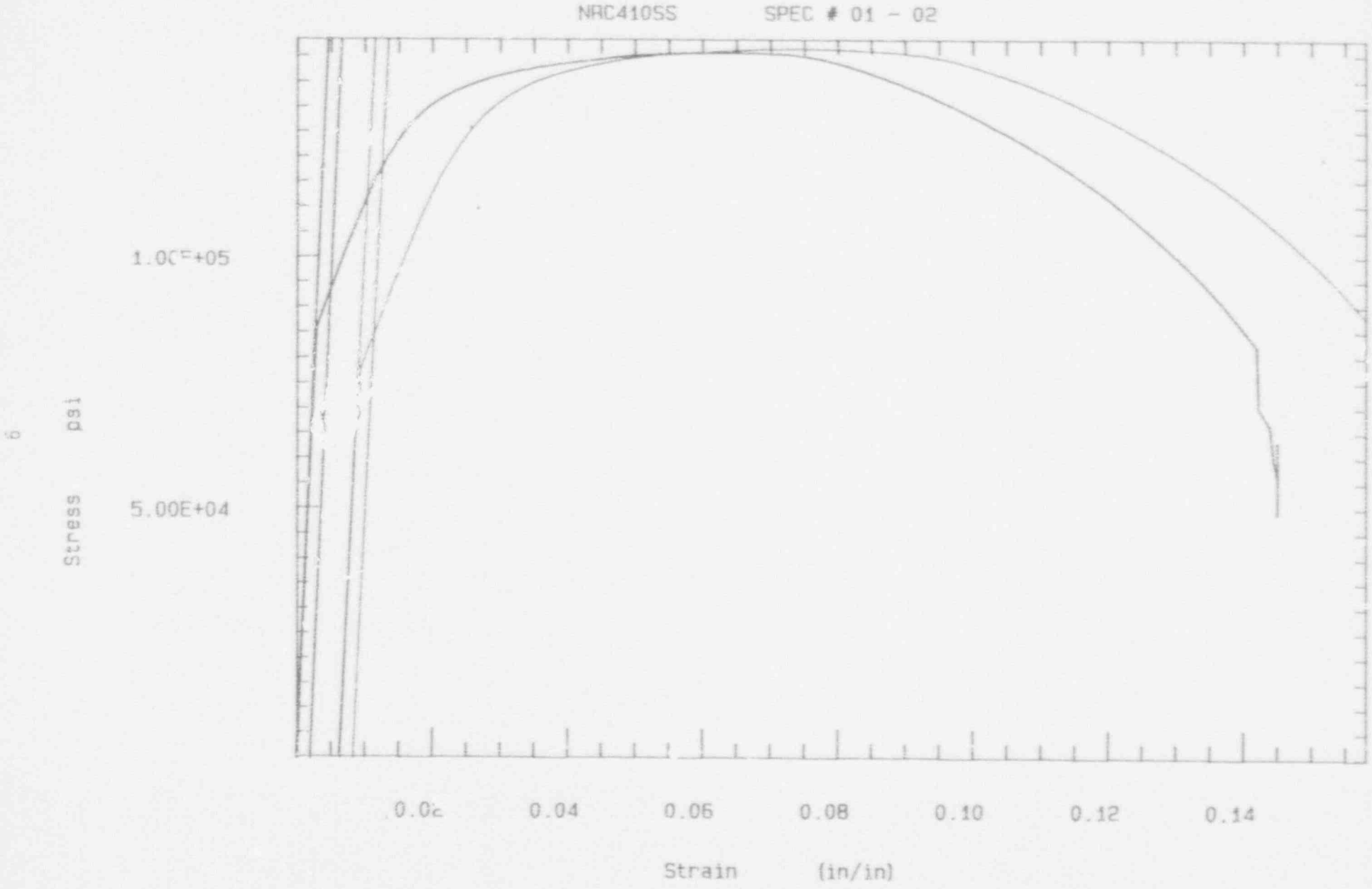

Figure 7 Stress-strain curves for specimens 1 and 2.

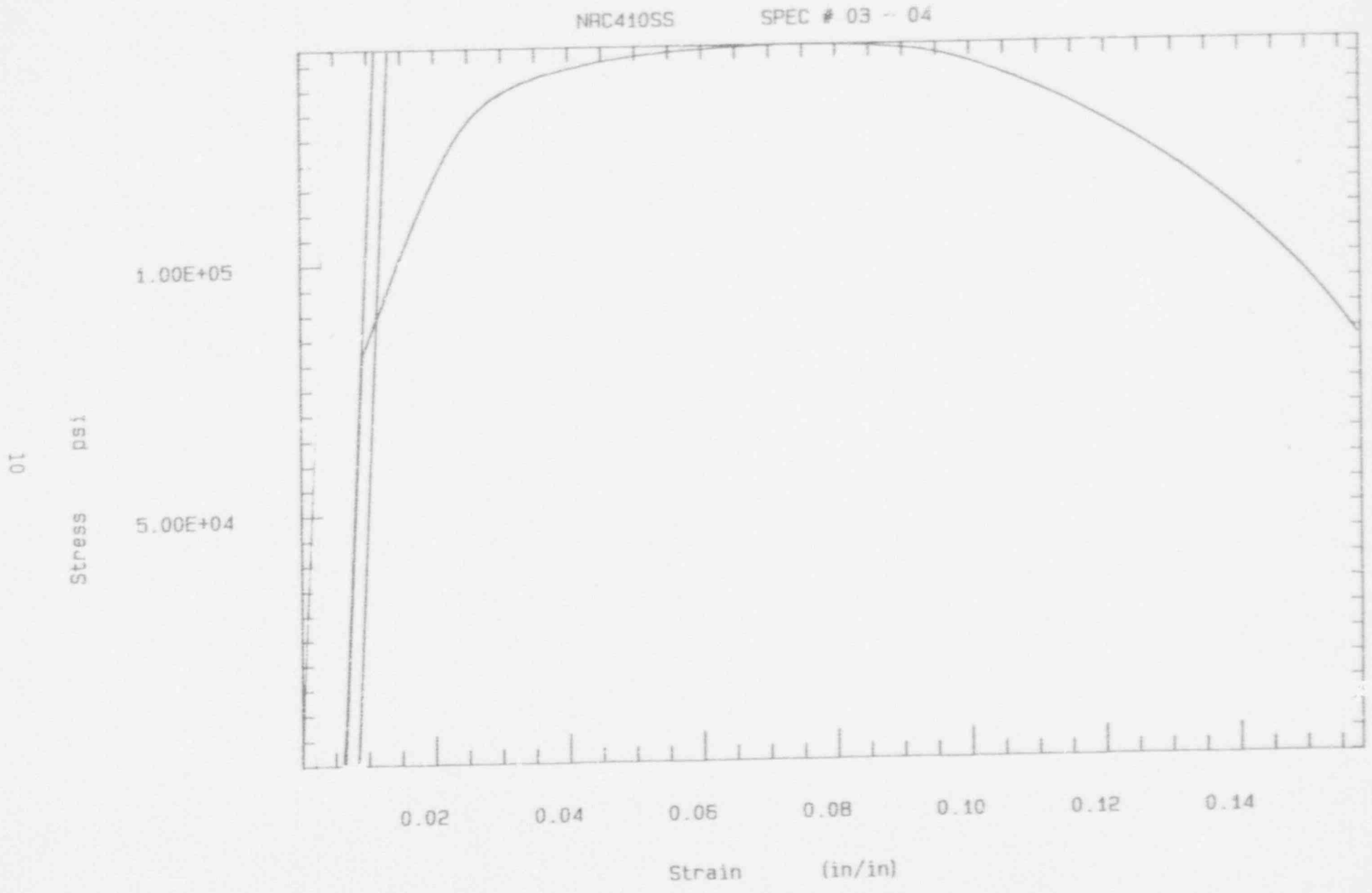

Figure 8 Stress-strain curves for specimens 3 and 4.

rupture) is present on both of the specimens. The secondary cracking and decohesion of apparent grain boundaries are a clear indication that the material was somehow embrittled.

Charpy Impact Testing

A total of eight subsize charpy impact specimens were machined from the coupling. Specimens C1-C3 were tested "as received"; C4 - C6 were tested after vacuum degassing for 48 hours at 200°C and C7 and C8 were tested after heat treating the specimens to 1300°F for 1 hour and then oil quenching. Table 4 list the results of these tests:

Table 4 Charpy Impact Test Results

Specimen #	Length (in.)	Width (in.)	Thickness (in.)	Absorbed Energy (ft-lbs)	Lateral Expansion (in)
C1	2.131	0.2950	0.394	10.0	0.0066
C2	2.126	0.2955	0.395	14.0	0.0126
C3	2.124	0.2960	0.395	15.0	0.0143
C4	2.126	0.2955	0.394	15.0	0.0122
C5	2.131	0.2950	0.394	11.5	0.0116
C6	2.125	0.2950	0.3945	8.0	0.0065
C7	2.118	0.295	0.3935	*DNF on 100ft-lb scale	
C8	2.118	0.295	0.3945	120	0.078
*DNF - Did Not Fail					

There was no apparent difference in absorbed energy between the "as received" specimens (C1, C2, C3) and the vacuum degassed specimens (C4, C5, C6). There was, however, an eight fold increase in absorbed energy after the specimens were heat treated and oil quenched. There was also a six fold increase in lateral expansion after the heat treatment.

The fracture faces of specimens C1, C2, C4, C6, C7, and C8 were examined by the SEM after testing.

The "as received" and the vacuum degassed specimens (C1, C2, C4 and C6) were virtually 100% intergranular with no apparent area of shear fracture (Figures 11a - 14b).

The cracked impact specimen C7 was submerged in liquid nitrogen and then broken apart. After warming to room temperature, the fracture face of C7 was examined in the SEM. Figures 15a - 15c show the results of this examination.

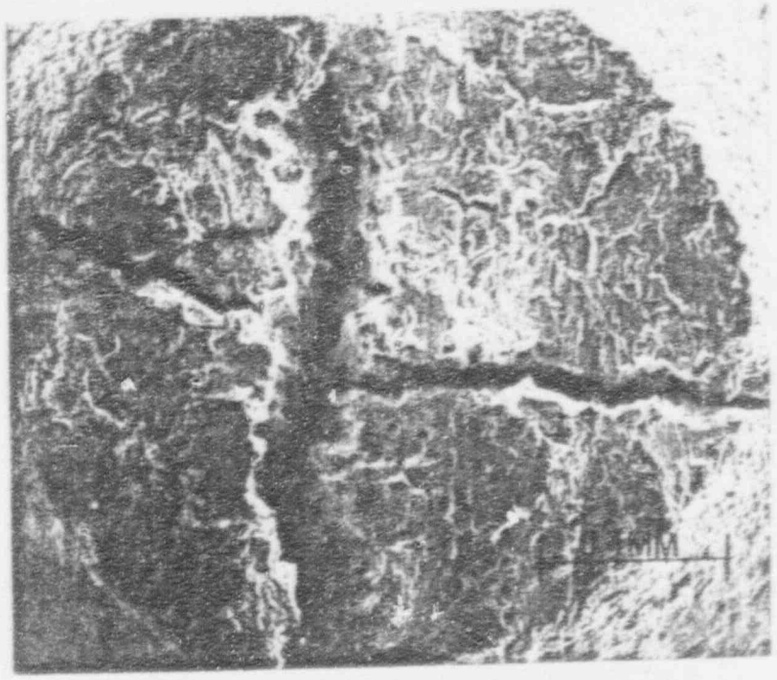

Figure 9a SEM photo tensile specimen 1.

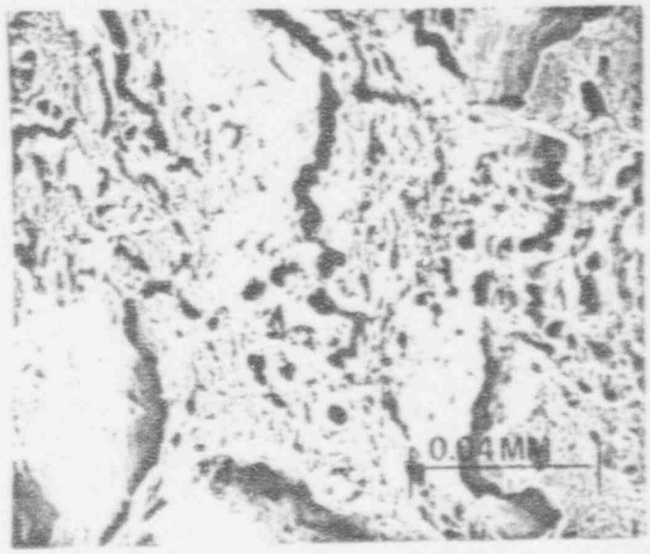

Figure 9b Grain boundary decohesion is evident at higher magnification.

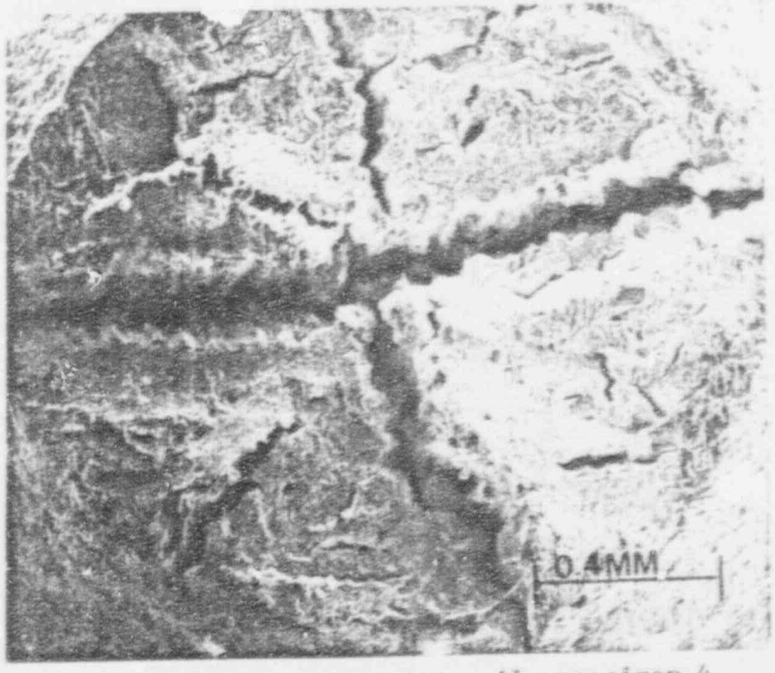

Figure 10a SEM photo of tensile specimen 4.

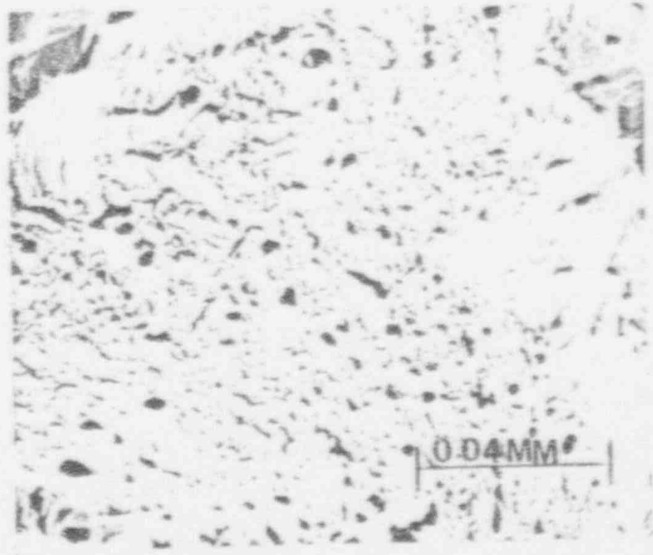

Figure 10b Higher maguification photo of specimen 4 show same type failure as seen in specimen 1 (Figure 9b).

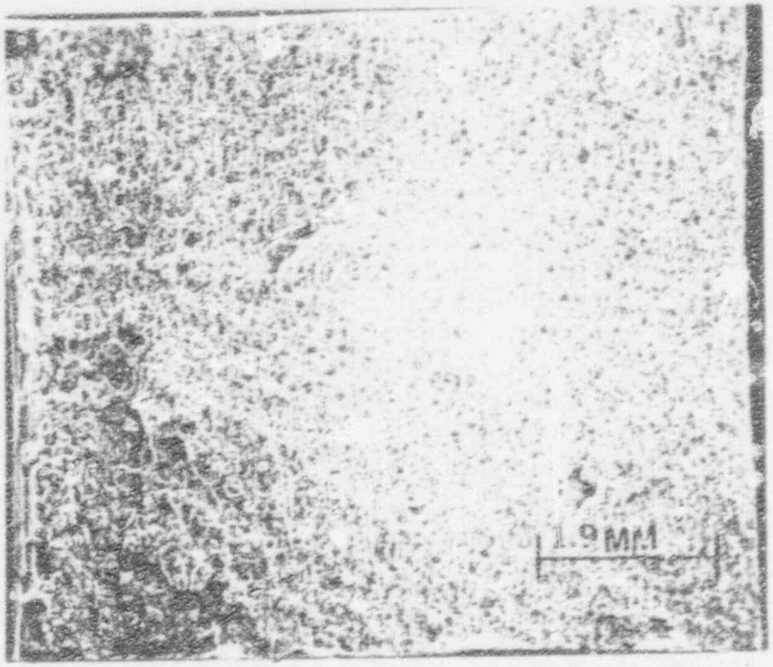

Figure 11a The fracture face for impact specimen C1 was essentially all intergranular.

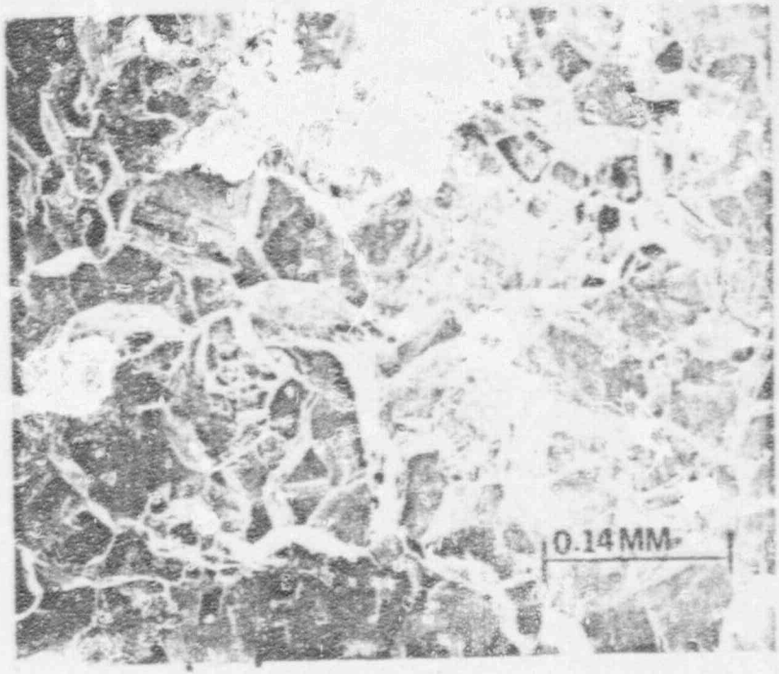

Figure 11b Higher magnification fractograph showing intergranular features.

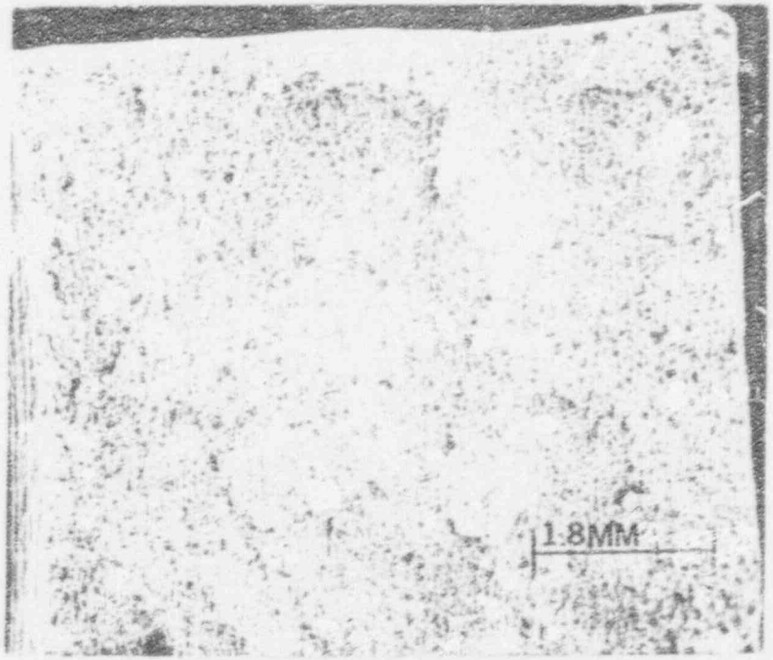

Figure 12a The fracture face of C2 was also intergranular.

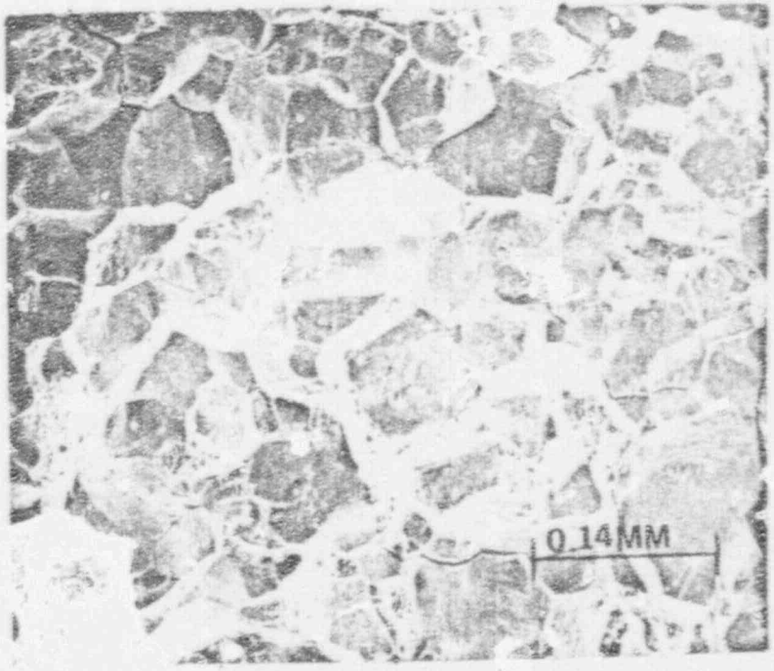

Figure 12b Higher magnification fractograph of C2.

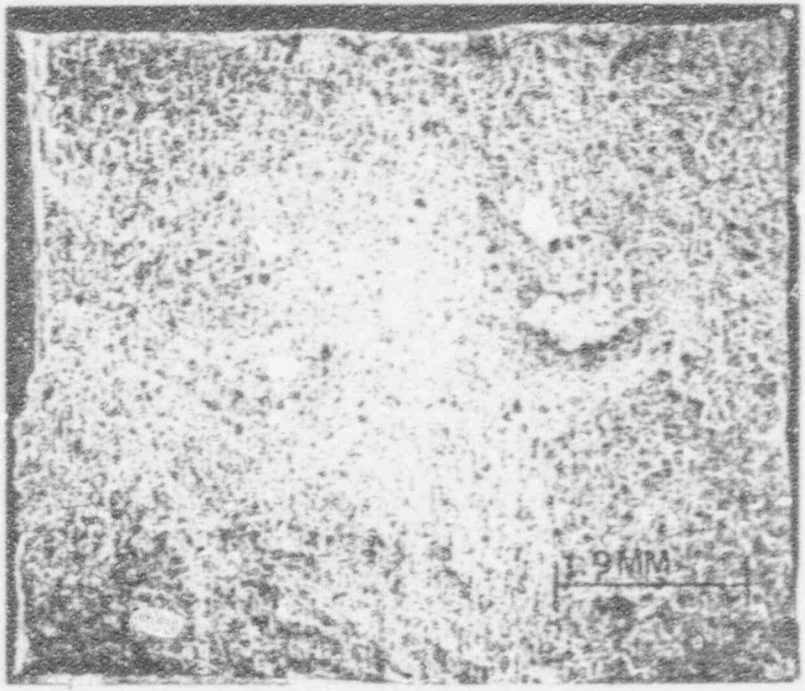

Figure 13a C4 fracture face was also intergranular.

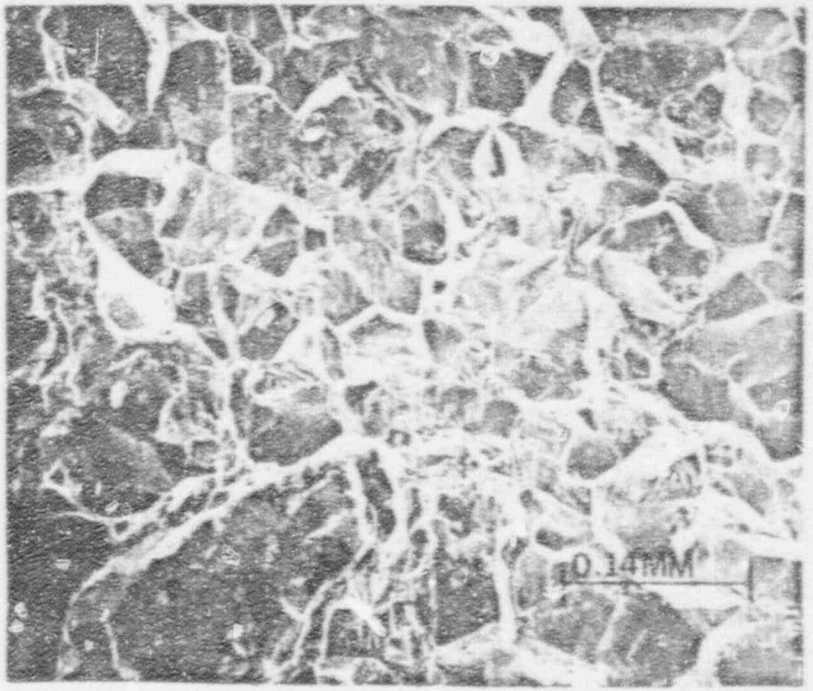

Figure 13b Intergranular facets are clearly evident on C4.

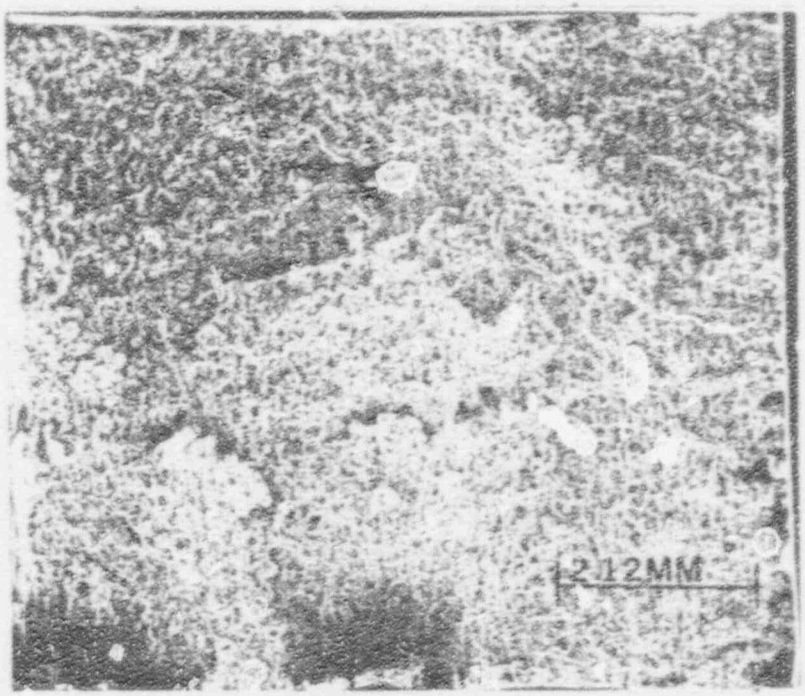

Figure 14a C6 fracture face was also essentially all intergranular.

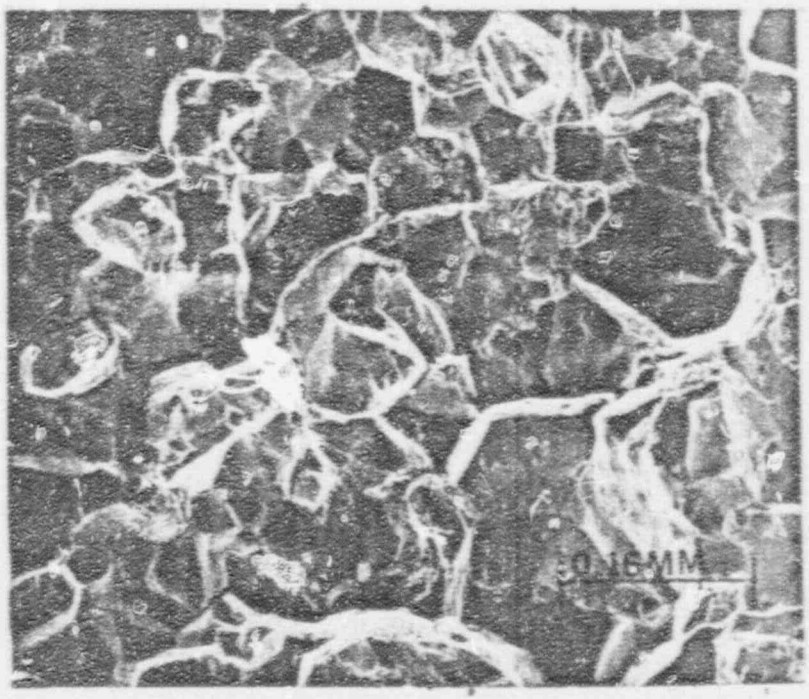

Figure 14b Higher magnification fractograph of C6.

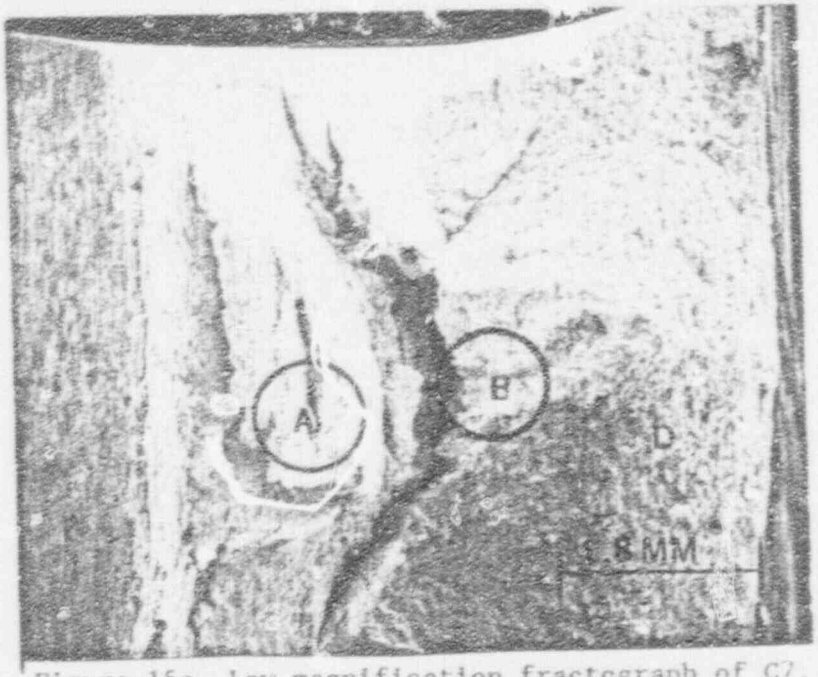

Figure 15a Low magnification fractograph of C7.
Area A - Shear fracture;
Area B - quasi cleavage area
broken at liquid N_2 temperatures.

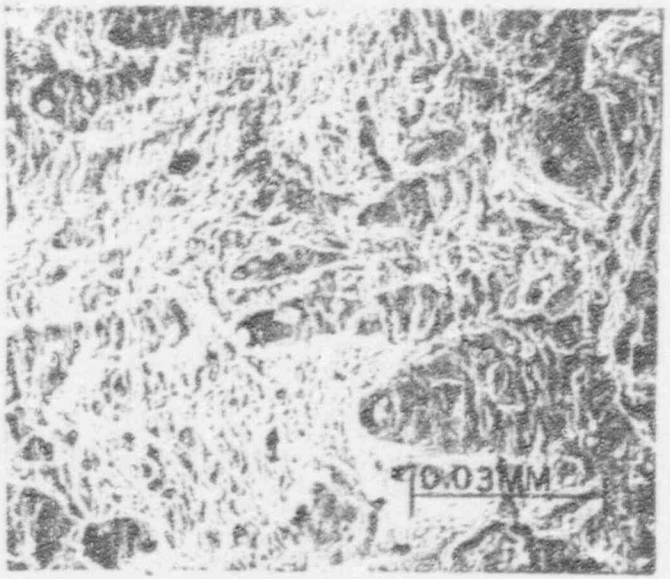

igure 15b Dimpled rupture failure is characteristic of Area A.

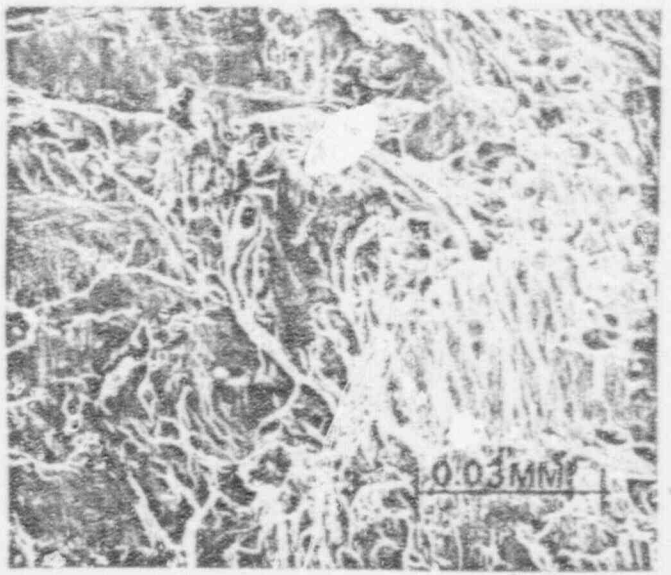

Figure 15c Quasi-cleavage failure of Area B was typical.

This specimen displayed a shear fracture for all of the specimen which broke in the impact test (Figure 15b) with the remainder of the specimen (Figure 15b) exhibiting quasi-cleavage failure as a result of the liquid nitrogen immersion and subsequent separation.

This dimpled rupture shear fracture was also found on specimen C8. Virtually all of the fracture face (over 90%) failed by shear (Figures 16a and 16b). This is a clear indication that the embrittlement process is reversible.

Since temper embrittlement was a distinct possibility as the cause of the failure, a section from specimen C2 (as received) and a section from C8 (1300°F heat treatment and oil quench) were mounted, polished and etched in Ethereal Picral etch [1].

This particular solution etches prior austenite grain boundaries of low alloy steels (temper-brittle condition) when the temper brittle condition results from the segregation of impurities to the prior austenite grain boundaries.

The etchant is prepared in the following manner:

Picric acid	50 grams
Purified ethyl ether	250 milliliters
Zephiran chloride (12.8% solution)	10 milliliters
Water	240 milliliters

The solution is prepared by dissolving the picric acid in ether and then adding the 250 milliliters of Zephiran-water solution. The resulting mixture is thoroughly shaken up. The solution must be kept in a tightly stoppered bottled to prevent excessive evaporation of the ether. After standing, the mixture separated into two layers, the top layer consisting essentially of a saturated solution of picric acid in ethyl ether containing Zephiran, and the bottom layer consisting of an aqueous Zephiran-picric acid solution.

The freshly prepared solution is allowed to stand overnight prior to use. After the first thorough shaking, no further agitation is necessary. To etch the metallographically polished specimens, decant a portion of the top layer into a small beaker, and dilute with approximately one-third by volume of ether.

After immersion of the specimens for 7 minutes, they were examined by visible light microscopy. Initial examination of the section from specimen C8 (1300°F heat treatment and oil quench) showed no evidence of grain boundary etching at two magnifications 100X (Figure 17a) and 300X (Figure 18a). This is contrasted to the etching in evidence at similar magnifications for the "as received" specimen from C2 (Figures 17b and 18b).

The same results were seen on the two samples after 14 minutes of etching (Figures 19a - 20b). It is evident that the etchtant has the effect of highlighting the grain boundaries of embrittled martensitic 410 stainless steel, but by what exact mechanism is yet unclear. Further research should be carried out to determine if this etch can provide a consistent nondestructive test for temper embrittlement in these steels.

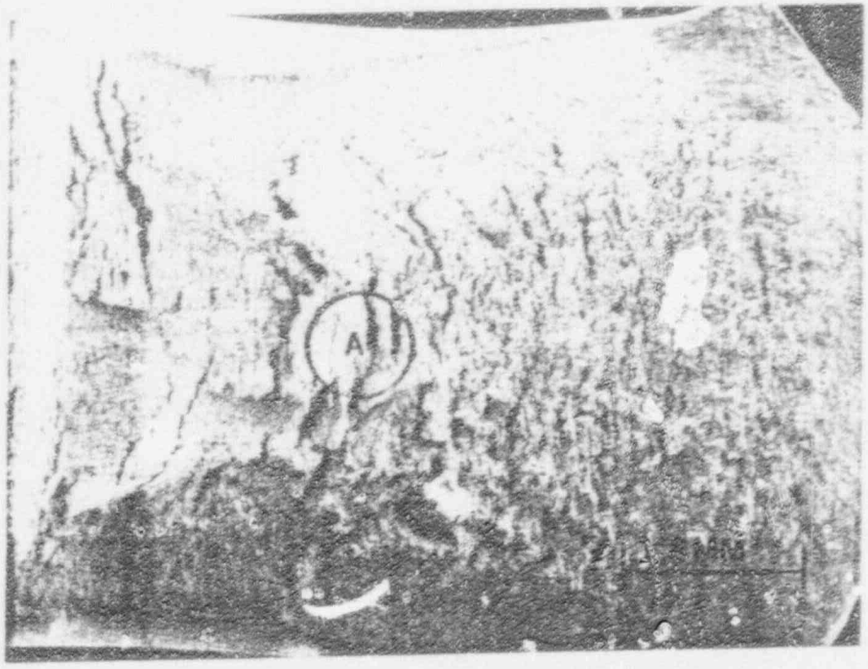

Figure 16a The fracture face for C8 was almost entirely a shear fracture.

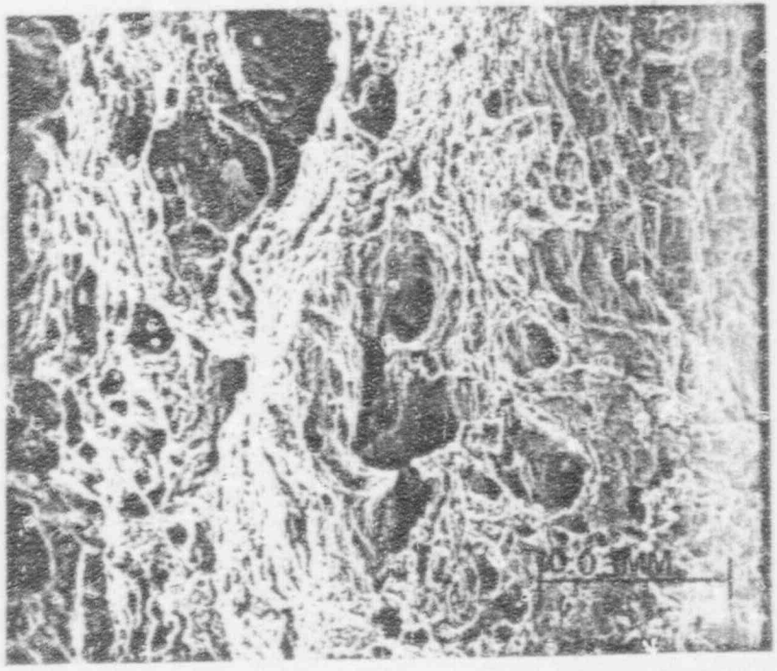

Figure 16b The ductile nature of the fracture is evident in this higher magnification fractograph of C8.

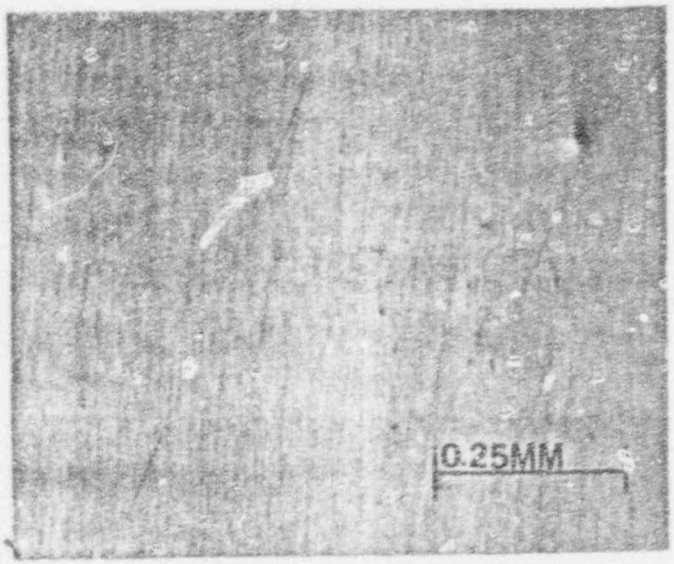

Figure 17a Low magnification photomicrograph from sample C8 - no grain boundary etching (7 minutes).

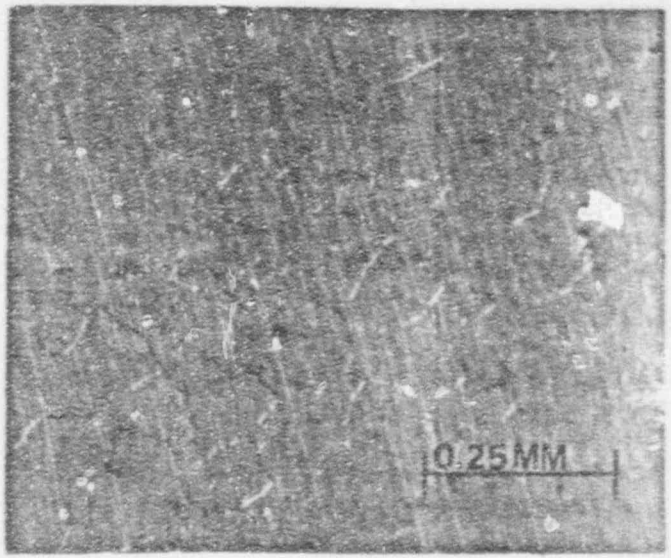

Figure 17b Grain boundary etching is evident on sample C2 specimen.

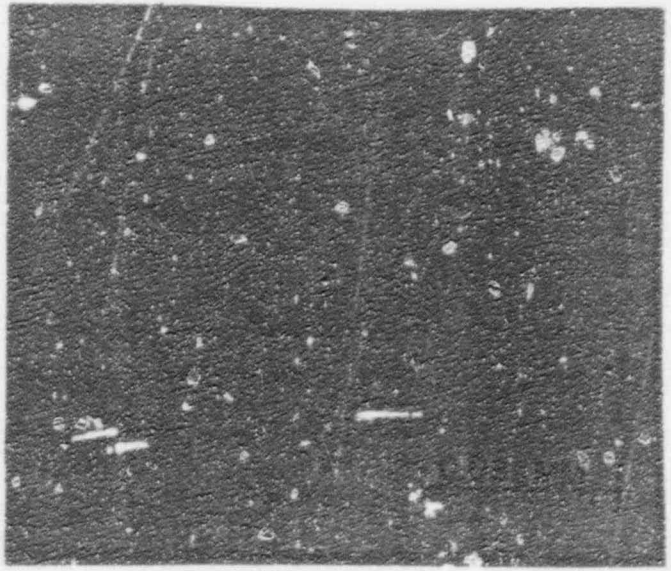

Figure 18a No evidence of grain boundary etching at higher magnification on C8 (7 minutes).

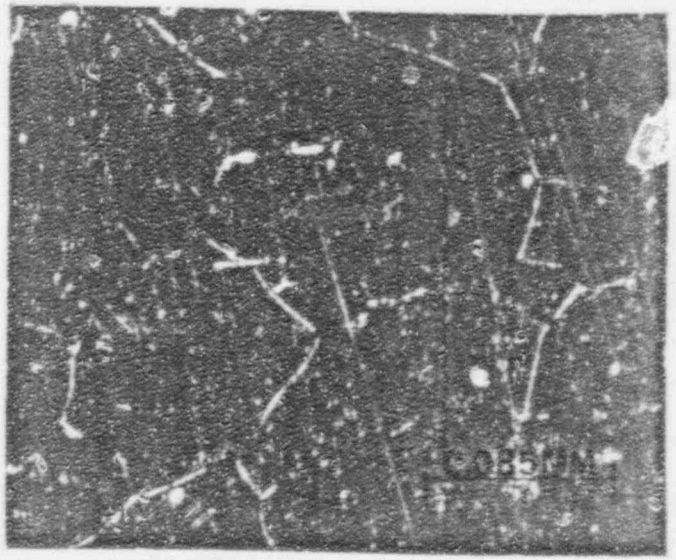

Figure 18b Grain boundaries are clearly delineated on sample C2.

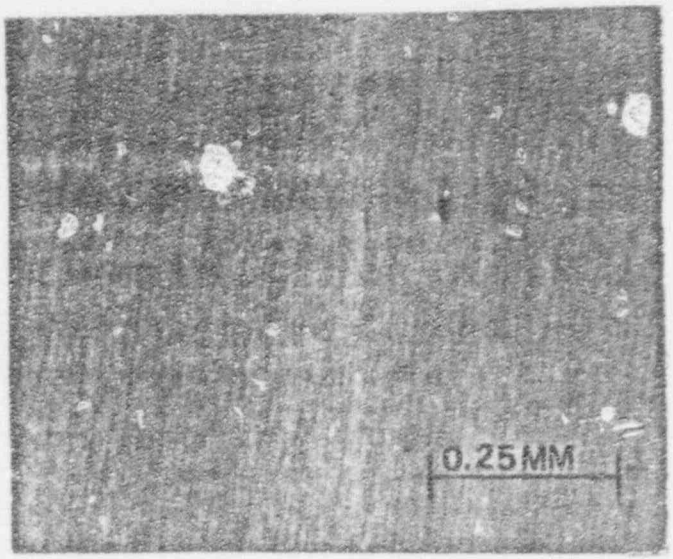

Figure 19a Fourteen minutes of etching did not reveal grain boundaries on specimens from C8.

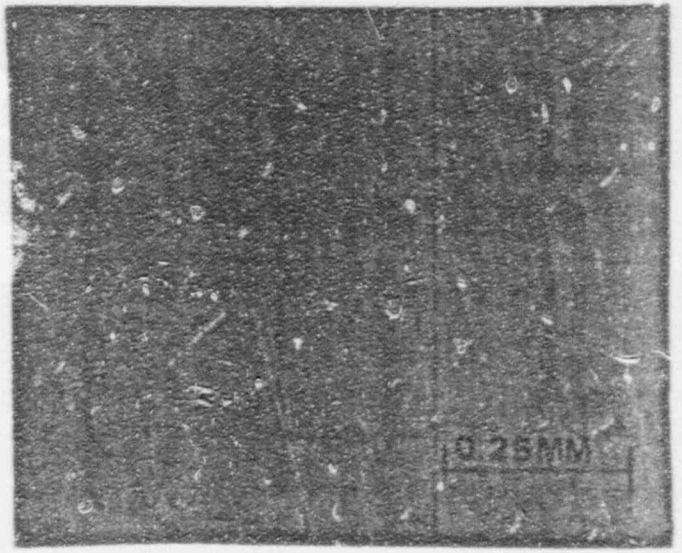

Figure 19b Grain boundaries are seen on C2 after 14 minutes of etching.

Figure 20a Higher magnification photo showing no boundary etching.

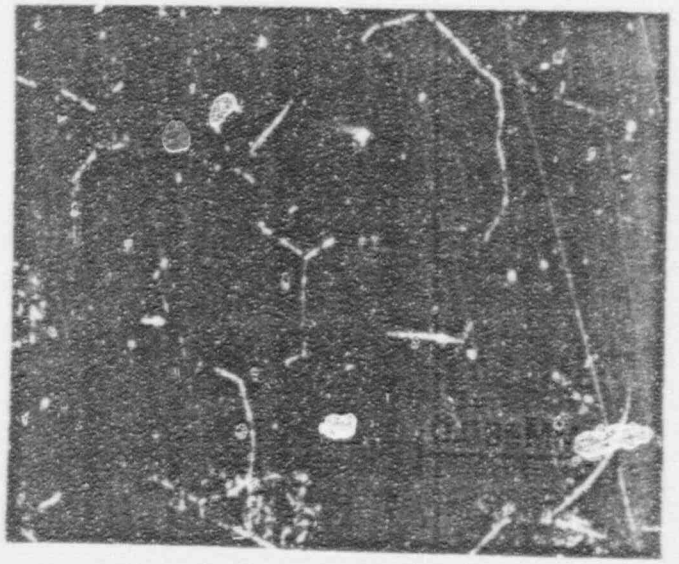

Figure 20b Grain boundaries are clearly seen on C2 at higher magnification.

6. DISCUSSION AND CONCLUSIONS

There are a number of ways that a tempered martensitic steel can suffer from an intergranular (brittle) failure. They are: quench cracking, stress corrosion cracking, hydrogen induced cracking, temper martensite embrittlement and temper embrittlement.

Quench/Heat Treatment Cracks

Quench/heat treatment cracking occurs from stresses produced during the austenite-martensite transformation when sufficient martensite has formed in the matrix to provide an internal stress sufficient to exceed the yield stress of the "as quenched" martensite [3]. Since there was no evidence of heat tinting on the observed fractures and no evidence of high temperature oxides, this mode of intergranular fracture is not considered probable.

Stress Corrosion Cracking (SCC)

Stress corrosion cracking occurs as a result of the synergistic effect of a susceptible material and tensile stresses (either applied or residual) in a corrosive environment. Stress corrosion cracks would normally grow until a critical flaw size is reached. After that point, fast fracture would be the predominant failure mode. Since this mechanism is time dependent it would fit the facts of the delay between the coupling's installation and subsequent failure. The low impact energies and intergranular fractures encountered in the coupling and reduced ductility of the 410 stainless steel give a clear indication that the material was embrittled and even though this type of cracking is possible, the degraded material properties of the 410 stainless steel tend to minimize this probability.

Hydrogen Induced Cracking

This type of cracking occurs in high strength steels which are normally under a sustained or slowly increasing load and which are exposed to environments where hydrogen is available to diffuse into the material. It normally occurs in ferritic alloys in the temperature range from -70°C to +140°C. The source of external hydrogen may be localized corrosion (simple Fe oxidation), H_2 pickup from plating operations or decomposition of hydrogen forming compounds (e.g. inclusions). Inclusions (MnS) promote hydrogen absorption by the matrix by acting as windows for hydrogen. Additionally, cracking is time dependent and occurs in the temperature range to which the coupling was exposed.

Since the 200°C vacuum degassing treatment on tensile specimens and charpy impact specimens (temperature which would drive off hydrogen, but not induce temper embrittlement) had no appreciable effect on the material properties of the coupling, this failure mode is considered unlikely. Additionally, hydrogen induced embrittlement normally would reduce the tensile strength of the material which did not occur with the coupling.

Tempered-Martensite Embrittlement

This type of embrittlement [5] occurs when steels are tempered in the range of between 250-400°C and causes a decrease in the steels toughness. This range of toughness decrease occurs at the same temperature where martensite begins its transformation to cementite and ferrite. The embrittlement from this mechanism

occurs along the grain boundaries where plate-like carbides precipitate. This carbide precipitation coupled with prior impurity segregation during the austenization process causes the intergranular embrittlement. The intergranular fractures on the impact specimens and the tensile specimens suggest this type of embrittlement. The mechanical properties evident in the "as received" coupling does not, however. 410 material tempered in this range has a tensile strength of 180-195 ksi with associated Rockwell "C" hardness in the range of 39-41 [2]. This was not the case, so this type of embrittlement is also discounted.

Temper Embrittlement

If a low alloy steel is quenched to form martensite and tempered between 600-700°C and then allowed to age at temperatures below 600°C; segregation can occur in the steel to the point where the ductile/brittle transition temperature will be raised, and intergranular failure is possible at room and higher temperature.

It has been recorded [5] that the elements phosphorous, tin and antimony segregate to the grain boundaries and cause this embrittling effect. In Cr-Mo steels, the major embrittling agent is phosphorous. Since the ethereal picral etch used during the metallographic portion of this evaluation is extremely sensitive to phosphorous and it indicated probable grain boundary segregation; this type of embrittlement is considered highly likely. This evidence coupled with the typical tensile and yield strengths recorded and the significant increase in mechanical properties after heat treatment and oil quenching greatly enhance the likelihood of this type of embrittlement being the cause of the failure.

The previous metallurgical investigation and literature review have resulted in the following conclusions:

1. The chemical analysis of the Beaver Valley riverwater coupling verified that the coupling was made from 410 stainless steel.

2. The observed cracking was intergranular and appeared to follow prior austenite grain boundaries in the tempered martensitic alloy matrix.

3. There was no evidence of heat tinting and no high temperature oxides present on the fractures. This precluded the possibility of heat treat cracking.

4. The mechanical properties were reasonably consistent for a 410 stainless steel tempered at 1000°F. There was a reduction in ductility and yield strength from expected values. The impact energy of the "as received" coupling material was extremely low (8 to 15 ft.lbs.) and was markedly increased (+100 to 120 ft.lbs.) after a corrective heat treatment was performed.

5. A new application of ethereal picral etchtant to 410 stainless steel may provide a nondestructive method of determining temper embrittlement in these steels, but more research is needed.

6. The root cause of the failure is considered to be temper embrittlement of the 410 stainless steel coupling brought about by improper heat treatment of the coupling during manufacture.

7. REFERENCES

1. Cohen, J.B., Hurlich, A., Jacobson, M., Transactions of the A.S.M., Volume 39, 1947, pages 109-138.

2. Metals Handbook, Eighth Edition, Volume 1, 1975, page 414.

3. Metals Handbook, Eighth Edition, Volume 10, 1975, page 74.

4. Engel, L., Klingele, H., An Atlas of Metal Damage, translated by Stewart Murray, Prentice-Hall, Inc., 1981, page 121.

5. Briant, C.L., Banerji, S.K., "Intergranular Fracture in Ferrous Alloys in Nonaggressive Environments," Treastise on Materials Science and Technology, Volume 25, Embrittlement of Engineering Alloys, Academic Press, 1983.